Experimental Wave Cancellation using a Cycloidal Wave Energy Converter

Stefan G. Siegel
Department of Aeronautics,
US Air Force Academy
United States
E-mail: stefan@siegels.us

Casey Fagley
Department of Aeronautics,
US Air Force Academy
United States

Marcus Römer
Department of Aeronautics,
US Air Force Academy
United States

Thomas E. McLaughlin
Department of Aeronautics,
US Air Force Academy
United States

Abstract—The ability of a Cycloidal Wave Energy Converter (CycWEC) to cancel deep ocean waves is investigated in a wave tunnel experiment. A CycWEC consists of one or more hydrofoils attached eccentrically to a shaft that is aligned parallel to the incoming waves. The entire device is fully submerged in operation. Wave cancellation requires synchronization of the rotation of the CycWEC with the incoming waves, as well as adjustment of the pitch angle of the blades in proportion to the wave height. We describe the development of a state estimator and controller that achieves this objective, using the signal from a resistive wave gage located up–wave of the CycWEC as input. The CycWEC model used for the present investigations features two blades that are adjustable in pitch in real time. The performance of the control scheme is demonstrated over a range of wave heights as well as periods. We achieve wave cancellation efficiencies as determined by wave measurements of greater than 85% for the majority of the cases investigated, with wave periods varying from 0.4s to 0.75s and wave heights ranging from $\approx 5mm_{pk}$ to $\approx 20mm_{pk}$ at a model scale of 1:300. The range of wave periods investigated covers both deep and intermediate water waves, while the wave heights range from small height linear Airy to 3rd order Stokes waves. We thus conclude that the CycWEC can efficiently interact with waves of varying height and frequency, which is in good agreement with earlier results obtained from numerical simulations.

Index Terms—Wave termination, Cycloidal Wave Energy Converter, Feedback Control, Deep Ocean Wave, Wave Tunnel

I. Introduction

Among alternative energy sources, wave power is one of the most abundant sources on earth. The World Energy Council according to [1] has estimated the world wide annual amount of wave power energy at 17.5 PWh (Peta Watt hours = $10^{12}kWh$). This amount of power is actually comparable to the annual world wide electric energy consumption, which is currently estimated at 16 PWh. Thus, wave power has the potential to provide a large portion of the worlds electric energy needs, if it can be harnessed efficiently. In addition to the energy availability, wave power has other advantages. Since a large portion of the worlds population lives close to the ocean shores, the distance between energy production and consumption is small, which reduces transmission losses and necessary investments in transmission lines. As opposed to other alternative energy sources like wind, stream and solar energy, the installation of wave power devices does not require use of already precious real estate. This makes wave power an ideal energy source for efficiently providing renewable energy to densely populated coastal areas. Ocean waves have a tremendous potential to provide clean renewable energy. Further engineering aspects of wave power as an energy source are appealing as well. While the power density of both solar and wind in typical favorable sites is in the order of $1kWm^{-2}$ [2], wave power in a typical North Atlantic wave that was considered in a related paper [3] (wave height of $H = 3.5m$ and period of $T = 9s$) yields $108\ kWm^{-1}$ of wave crest. As shown there, a device extending about $40m$ in the vertical direction can extract almost all of this wave power, yielding a power density of about $2.7kWm^{-2}$ or more than two and a half times that of wind or solar power. If one considers the theoretical inviscid conversion limits for waves and wind, which are 100% for waves [4] and 59% for wind [5], the accessible power density of waves is more than four times as large as that of wind. Furthermore, wave energy is available on a more consistent basis and can be better predicted in advance, therefore mitigating the need to back up a wave power plant with other conventional power sources, such as solar and wind energy.

II. Motivation and Objectives

Analysis of the different wave energy conversion devices that have been investigated or proposed reveals a number of commonalities in design. The first is that all devices require a connection to the sea bed in order to extract energy, which has two main drawbacks. First, a seabed connection makes the device vulnerable in rough seas and storms, in the same way as an anchored ship is vulnerable in a storm (and will likely break the anchor line). According to [1], storm survivability has been a major problem for many wave energy converters, with some being destroyed by the elements as early as during deployment. Also, for most of the devices, the load imposed onto the seabed connection is proportional to the power which the device can extract. This means that the anchor point needs to be stronger and thus more costly as more energy is being extracted. Therefore, many of these devices cannot easily be scaled up to industrial power plant levels of energy conversion. In addition, since the devices need to be anchored to the sea floor, they are not well suited to operation in deep water waves, where the ocean floor may be hundreds of meters away from
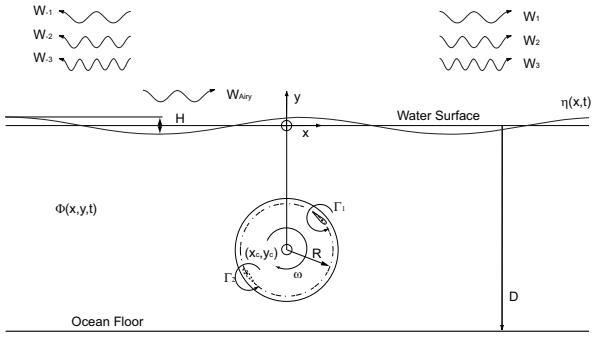
Fig. 1. Cycloidal wave energy converter geometry and generated waves

the surface. However, most wave energy is contained in deep water waves, and the energy density of a wave decreases as it approaches shallow water. Thus, most devices cannot operate in the most promising locations for wave power extraction.

Beyond survivability, efficiency has been a major issue for many WEC designs. While wave energy as a resource may be free, the construction effort to harness it is a major expense and to a large degree determines the cost of energy being produced. As a less efficient WEC will need to be larger in size to extract the same amount of energy as a more efficient one, cost of energy is directly related to efficiency. Arguably, the most efficient WEC is one that can extract all of the energy from an incoming wave, and the class of wave energy converters that is able to achieve this is commonly referred to in literature as wave termination devices. There have been various wave termination designs reported in literature, with the most well known devices being the Salter Duck [6] and the Bristol or Evans Cylinder [7]. Both consist of a series of elements which are aligned parallel to the wave crests, in the case of the Salter Duck these are cam–shaped and floating on the surface, while the Bristol Cylinder is fully submerged. Both have been shown to be able to absorb an incoming wave completely. The wave energy is converted to electric power by means of a power–take–off system that is hydraulic in both cases. As both devices move at approximately the wave induced water velocity, the devices need to feature a large surface area to convert appreciable amounts of power. This increases construction cost, reduces storm survival odds and has ultimately motivated the investigation of the Cycloidal WEC described here. The fact that both devices require mooring to the ocean floor also hampers storm survival odds and precludes installation in very deep water.

A typical cycloidal wave energy converter (CycWEC) as considered in this paper is shown in figure 1. It features one or more hydrofoils attached eccentrically to a main shaft at a radius R. While the shaft rotates, the pitch angle of the blades may be adjusted. This device operates at a rotational speed of the hydrofoil that is typically an order of magnitude larger than the wave induced water velocity, and employs the lift force at the hydrofoil to generate shaft torque directly. Using lift allows for a much smaller hydrofoil planform area to be employed compared to the cross sectional areas of Duck and Cylinder,

and generating shaft torque directly eliminates the need for a costly and inefficient hydraulic power take off system. In addition, it is conceptually possible to join several CycWECs into a cluster where the reactive forces at the shaft can be made to cancel, which reduces or negates entirely the need for mooring and thus enables deep water deployment while improving storm survival odds (see Siegel [8] for sketches). A single rotating hydrofoil was first investigated by Hermans et al. [9] both numerically and experimentally. While Hermans et al. reported very low wave energy conversion efficiencies (on the order of a few percent), Siegel et al. [3] were able to show in simulations that with improved sizing of the WEC as well as using feedback control to synchronize the rotation of the foil with the incoming wave, wave termination with better than 99% inviscid efficiency is possible. These numerical findings were confirmed by 1:300 scale experiments earlier this year, as reported by Siegel et al. [10] where invisicid conversion efficiencies of greater than 95% were achieved.

These successful wave termination simulations and experiments are continued in the present study. While feedback controlled wave termination based on a up–wave sensor signal was always envisioned, both [3] and [10] employed synchronization instead of feedback control. While much simpler to implement, synchronization requires a priori knowledge of the incoming wave height, amplitude and phase. This is information that is available in simulation and controlled laboratory experiment, but not in any actual ocean setting. Thus, deployment of the CycWEC requires both state estimation and feedback control capabilities. In the present paper, we describe development of both of these components for the same experiment that was reported in [10]. With feedback control successfully implemented for the design wave, we demonstrate in a parameter study that the CycWEC can efficiently cancel incoming waves spanning a range of wave periods and wave heights.

III. EXPERIMENTAL SETUP

The tunnel used for testing the cycloidal WEC was a 2D wave tunnel designed to provide a 1:300 scale model of a deep ocean wave. The full scale design deep ocean wave, which was investigated numerically in [3] had a period of 9s, a wave length of 126.5m and a wave height of 3.5m, and it carried about 105kW of power per meter of wave crest. It was represented in the present setup by a wave with a period of 0.5s and wave length of 0.39m; at a typical wave height of 20mm the scaled wave carried approximately 192mW of wave power per meter. The experiment consisted of four subparts: Wave tunnel, CycWEC model, wave gages and Data Acquisition (DAQ) and processing system. In addition, a feedback controller and state estimator were employed to operate the CycWEC. All of these components are described in detail in the following subsections.

A. Wave Tunnel

The wave tunnel is shown as conceptual sketch in figure 2. It allowed for the generation of waves with a period between

0.2 and 1.15 seconds, and consisted of the following three parts:

1) The wave tank: The tank had an overall length of 5m, where 4.50 meter were usable for wave experiments between the flap wave maker and the beach, a width of 0.55m and a design water depth of 0.3m. The width of the tunnel was increased by 50mm on each side in the center test section, which allowed the drive system of the CycWEC to be placed outside of the wave testing area by means of false walls. The eigenfrequency of the wave tunnel had a period of 5.5-6 seconds, which was determined by exciting the tunnel resonance using a step input at the wave maker.

2) The beach: The beach, located at the right end of the tunnel, was a linear beach with a 1:4 slope. The main purpose was to prevent reflection of waves traveling left to right. In order to evaluate the wave reflections from the beach, the reflection coefficient was measured experimentally and also compared to predictions based on a well established numerical model. At the design wave of $T = 0.5s, H = 20mm$ the reflection coefficient was measured by traversing two wave gages using the approach described in [7] and found to be $C_r = 0.106$. This was less than the estimate from the numerical model described in [11], which for the design wave estimated the reflection coefficient to be $C_r = 0.17$ which is the ratio between reflected and incident wave. We thus considered the numerical model a worst case estimate, and given textbook statements that consider it difficult to achieve less than $C_r = 0.1$ [12] the beach was found to perform sufficiently well for the measurements at hand. No wave reflection prevention (e.g. wave canceling wave maker) was available at the left end of the tunnel for waves traveling right to left, where the flap wave maker was located. This did not cause any significant impact on the results, though, since the wave heights on the up–wave side of the WEC model were minimal for all data presented.

3) The flap wave maker: The flap wave maker was a plain flap hinged at the bottom of the tunnel. It was driven by a brush type servo motor driving two sprockets attached to a shaft spanning the tunnel, which engaged in two arc gear segments located at both sides of the tunnel attached to the top of the flap. This setup provided gearing to match the torque characteristics of the servo motor to the torque requirements of the wave maker. It also ensured pure rotational motion of the flap without torsion. The servo motor was connected to a motion controller operating in position mode allowing for arbitrary motion wave forms with an update rate of 10ms. In the present investigations, a sinusoidal motion

$$\gamma(t) = \delta \sin(2\pi t/T) \qquad (1)$$

was prescribed using a deterministic hardware timed Lab-VIEW loop. This setup had the advantage that both wave height and period could be computer controlled without any hardware adjustments. It did not provide any incoming wave cancellation since no force feedback was available. Given the resolution of 2000 pulses per revolution of the servo motor
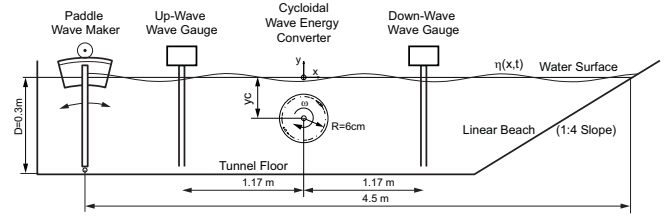
Fig. 2. Wave tunnel schematic - not to scale

shaft mounted encoder, and the gear ratio of 10:1 an angular resolution of 0.018 degrees was achieved.

Figure 2 shows a sketch of the overall test setup. The flap wave maker generated waves at the left side of the tunnel, which traveled past the first wave gage (up–wave wave gage). In the center of the test section the wave reached the CycWEC. The remaining waves were measured by the second wave gage, which was located at an equal distance from the CycWEC. After a short distance the waves dissipated their energy at the beach.

B. Wave Energy Converter Model

Based on the sketch in figure 1, a number of non–dimensional quantities emerged. The basic size of the wave energy converter was denoted by $2R/\lambda$, where the wave length λ was the fundamental length scale. Consequently, the vertical position of the main shaft was denoted by y_c, and the wave height by H. It was also convenient for parameter studies to compare different size wave energy converters while keeping the distance between the water surface and the topmost point of the cycloidal wave energy converter path fixed, that is $|y_c| - R = const$. The direction of travel of an incoming ocean wave W_{Airy} was assumed to be left to right. Waves generated by the cycloidal wave energy converter that travelled in the direction of the incoming wave received a positive index and were considered traveling down–wave; while waves in the opposite direction were considered up–wave traveling and received a negative index number.

The CycWEC device was designed to convert energy from waves to shaft power by wave cancellation. Figure 3 shows a CAD model, while the definition of the main geometry parameters is shown in figure 1. The only component interaction with the flow were two hydrofoils spanning the tunnel. These hydrofoils were attached eccentrically at a radius $R = 60mm$, and had a NACA 4 series hydrofoil of $c = 50mm$ chord length, with a camber line curvature to match the radius of the circle on which it rotated. The hydrofoil had a resulting camber line displacement of 11 percent, and the maximum thickness of 15% was located at 50% chord. This setup provided a zero–lift pitch angle of $\approx 0°$ and was expected to behave like the familiar NACA 0015 in straight flow, when rotating around a shaft.

The CycWEC was installed in the center of the wave tunnel such that the waves traveling the length of the tunnel were unobstructed but for the interaction with the CycWEC blades. The CycWEC could be operated with one or two blades,

however all results presented in this paper were obtained with two blades. The main shaft motor was located outside the water well above the tunnel, and connected directly to two timing belt sprockets. The timing belts engaged in individual larger sprockets below the water line with a 5:1 gear ratio, which in turn held the blades. The main shaft motor (Pittman model 4442 S012) was a brushless servo motor with a 500 lines/rev incremental encoder driving the main shaft directly, and connected to a closed loop servo motor controller (Copley Motion Accelnet ACJ-090-12) allowing the motor to operate both as motor or generator depending on the torque applied to the shaft. Together with the 5:1 gear ratio as well as edge detection of the encoder signals, an overall resolution of 10000 counts/revolution was achieved. The motor controller was operated in position mode, with position updates transmitted every 10ms to the controller over the CAN bus system (see below).

The pitch angle of each blade was adjustable under computer control in real time. This was achieved by means of two digital model aircraft servos, which were attached to the main shaft located outside the water. The servos turned a second timing belt sprocket by means of a gear attached to the servo shaft. The sprocket then adjusted the pitch of the blade by means of a second set of timing belts and 5:1 larger sprocket arranged concentrically with the drive sprocket, which connected to a push rod that was attached to the blade. The servos had a range of motion of $\pm 60°$, and with an overall gear ratio of 3:1 the blades could be adjusted over a range of $\approx \pm 20°$. The transmission also improved the positioning accuracy of the servos, which was measured to be $\pm 0.5°$, to one third of that, or $\approx \pm 0.17°$.

The sign convention for the pitch angle was chosen such that a rotation of the blade's leading edge towards the rotation center was negative, a rotation outward positive. For the present investigation, the blades were pitched in opposite direction at all times, which was found to provide the best performance in previous numerical studies.

The depth to which the rotational center of the WEC was submerged below the mean water surface, y_c, could be adjusted from the surface to $y_c = -0.1m$. This was achieved by adjusting the supports on both sides of the WEC model, and was estimated to be accurate to $\pm 0.5mm$. In accordance with findings from previous experimental investigations performed in the same facility, the submergence was kept constant in the present study at the optimal value of $|y_c| - R = 15mm$.

C. Wave Gauges

Two wire type wave gages for wave height measurements were placed at a distance of $1.17m$ up– and down–stream of the WEC main shaft. The measurement of water level was by electrical resistance measurement. The wave gages were operated with 2.5 V, 5khz AC and consisted of two stainless steel wires and a ground electrode. The signal from the wave gages was first filtered by a high-pass analog filter to remove any DC offset, then rectified and again low-pass filtered with a corner frequency of 200Hz before it was amplified and dig-
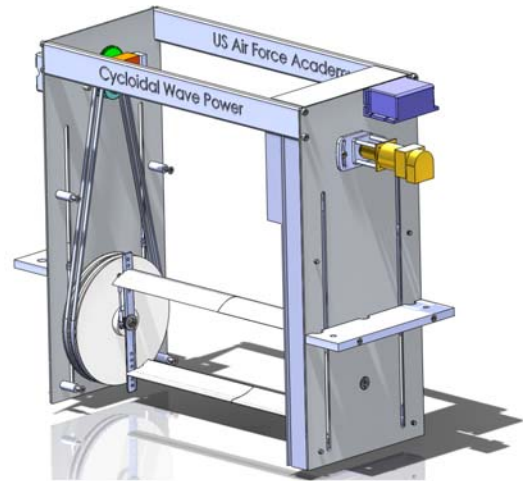
Fig. 3. Picture of wave energy converter with a two blades and pitch control.

itized by a 10 bit A/D converter. The resulting measurements were transmitted over the same CAN bus system that the main shaft controller employed, using CANOpen as the data protocol. The wave gages were calibrated for a measurement range of $y_m = \pm 50mm$ before each measurement session, and the calibration was repeated after the last measurement run to verify that no drift in calibration had occurred. The overall accuracy and repeatability of the wave gage measurements was estimated to be better than $\pm 0.1mm$ based on the repeat calibration results, or $\pm 0.5\%$ of the design wave height.

D. DAQ and Post Processing

The entire experiment was controlled by a WINDOWS XP PC, using software written in LABView to transmit data over the CAN bus (Controller Area Network) to operate the wave maker, the wave gauges and the CycWEC. The received data was stored in Matlab files for post-processing. The sample rate of the system was 100 Hz for both position control as well as data acquisition, where all transmitted messages where synchronized using the CANOpen sync messages. Every measurement lasted 61 seconds, but only the last 40 seconds when the flow had reached a periodic state were used for data analysis by means of Fourier transform to determine wave heights.

E. Feedback Control

A sketch of the overall control and estimation scheme is shown in figure 4. The signal from the up–wave wave gage is used for feedback control, and processed first by the state estimator. The results of the state estimation algorithm are the instantaneous wave height H, wave period T, and wave phase ϕ. These quantities are then used by the controller to prescribe the main shaft angle ϕ as well as the pitch of the blades. The following subsections describe the estimator and controller in more detail.
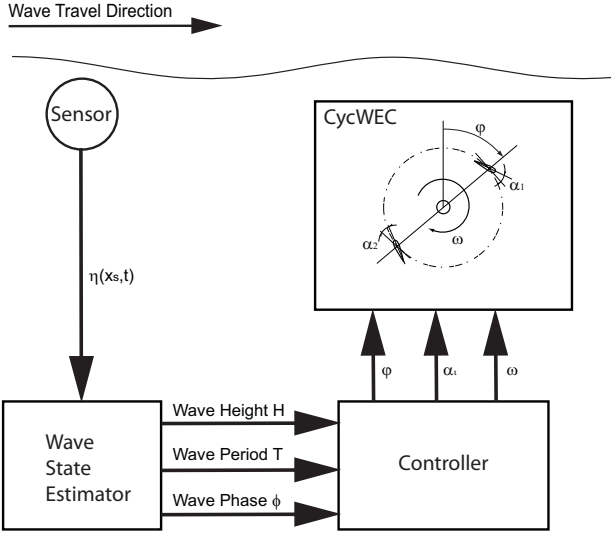
Fig. 4.   Block diagram of sensing and feedback control approach

For the successful cancellation of an unknown, incoming harmonic wave, feedback control and wave state estimation were necessary. Algorithms to interpret and estimate the wave state in real time fashion were needed to adequately control and efficiently extract energy. The wave state for a single airy wave was defined as phase ϕ, frequency ω, and wave height H. While different types of sensors which measures the water elevation over time may be employed, the wave gage that was placed upstream of the CycWEC was used in this study. This measurement was defined as $\eta(t)$ and displayed a periodic signal with unknown frequency and amplitude and was also corrupted by a small amount of high frequency noise. Given a time history of the upstream measurement a relation was sought such that $[\hat{\omega}(t)\hat{\phi}(t)\hat{H}(t)]^T = f([\eta(t), \eta(t-1), \ldots, \eta(t-n)]) + e(t)$ with minimal estimation error, $e(t)$. A typical Fourier analysis fell short because instantaneous phase information was lost in the decomposition. Other digital signal processing methods needed to be implemented.

Because the upstream wave height measurement contained no negative frequency components, the signal could be expressed as an analytic signal such that

$$\eta(t) = \frac{1}{2\pi} \int_0^\infty \eta(\omega) e^{j\omega t} d\omega \qquad (2)$$

A complex representation of a periodic signal is $e^{j\omega t} = \eta(t) + i\hat{\eta}(t)$. The complex component of the analytic signal, which was unknown at this point, was analogous to the Hilbert transformation, $\mathcal{H}[\bullet]$, of the real component; that is $\hat{\eta}(t) = \mathcal{H}[\eta(t)]$. The Hilbert transformation was a linear filter which produced a phase shift of $\pm\frac{\pi}{2}$ over all frequencies present in the signal, $\eta(t)$. In the time domain the transformation for this linear filter was identically the convolution with $\frac{1}{\pi t}$ which is shown as,

$$\mathcal{H}[\eta(t)] = \frac{1}{\pi t} * \eta(t) = \frac{1}{\pi} \int_{-\infty}^\infty \frac{\eta(t-\tau)}{\tau} d\tau. \qquad (3)$$

In the frequency domain the transform of the signal $f = \frac{1}{\pi t}$ is

$$-j\,sgn(f) = \begin{cases} -j & f > 0 \\ 0 & f = 0 \\ j & f < 0 \end{cases} \qquad (4)$$

The transfer function of this ideal filter did have a magnitude of one and a phase of $\pm\frac{\pi}{2}$ for $\pm\omega$, respectively. Now because the Fourier transform was a non-causal transformation (dependent on previous, current and future measurements), an approximation to this transformation was necessary. Typical filters such as finite impulse response (FIR) and infinite impulse response (IIR) filters could be designed to simulate the response of $\frac{1}{\pi t}$. For the purposes of this paper, a 3 stage cascading IIR filter was used to estimate the complex component of the Hilbert transformation with minimal (although non-linear) phase delays at the design frequency.

Now that the real and complex components of the analytic signal were known to within some degree of error, the instantaneous amplitude was estimated from the L_2 norm of the signals, i.e. $\hat{H}(t) = \|\eta(t) + \hat{\eta}(t)\|_2$. The instantaneous phase was then computed as the angle between the real and complex estimate as, $\hat{\phi}(t) = \arctan(\frac{\hat{\eta}(t)}{\eta(t)})$, and the instantaneous frequency was calculated by the time derivative of the phase estimate.

As seen in figure 4, the wave state is now fully estimated. The control scheme is very basic for the purposes of this paper. Proportional control is used for the blade pitch, such that $\alpha_i(t) = P_g \hat{H}(t)$. This is a reasonable assumption since the open loop wave generation results shown in Siegel et al. [13] display a very linear relationship between the circulation Γ and wave height H. In order to implement rotary control for the wave energy converter the group velocity C_g needs to be estimated and compensated for as a phase delay. The frequency of the passing wave obtained from the estimator and water properties make this a simple calculation. The time delays are then superimposed to control the rotational velocity of the main shaft in a stepwise fashion, such that $\phi(t) = \Phi(t) + \frac{\eta_\lambda}{C_g} + \theta_f$, where C_g is the group velocity of the wave, and θ_f is the phase compensation of the Hilbert transformation filter.

IV. Results

The experiments in this study were conducted in two stages. First, experimental runs were performed at the design point of the wave energy converter and a moderate amplitude, i.e. a wave period of $T = 0.5s$ and a wave flap maker deflection of $\delta = 1.5°$. Throughout this first set of experimental runs, the optimal feedback phase θ and pitch gain G_p were optimized individually. The second set of experiments concerned a parameter study where the wave period and height of the incoming wave were varied, without changing any of the feedback parameters.

A. Wave Cancellation Pictures and Data

In this section, we first present pictures and data from a typical feedback controlled wave cancellation run, before

Fig. 5. Picture of wave cancellation from side. Incoming wave period $T = 0.5s$, flap wave maker amplitude $\delta = 1.5°$, WEC has two blades, feedback phase $\theta = 197°$, blade pitch gain $G_p = 400°/m$, submergence $|y_c| - R = 15mm$.
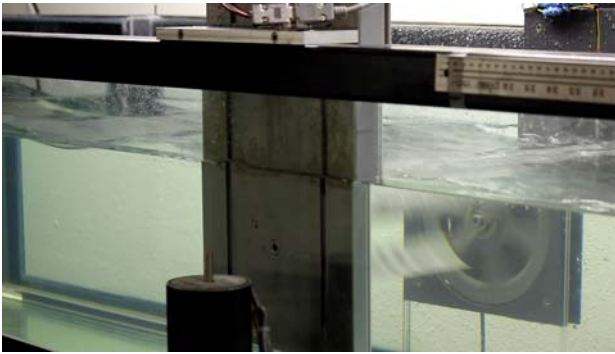
Fig. 6. Picture of wave cancellation from downwave above. For experimental parameters see caption figure 5

outlining the detailed results from the parameter studies in the following sections. A side view as well as a view of the experiment from above are shown in figures 5 and 6, respectively. The incoming wave, which is traveling left to right in both pictures, can be observed to be of large wave height up–wave of the CycWEC, and greatly reduced wave height down–wave of the CycWEC.

Wave gage data from a typical feedback controlled experiment run, as observed by the up–wave and down–wave wave gauges, is shown in figures 7 and 8. The flap wave maker is started at time $t = 0s$, and the feedback controller is activated at time $t = 10s$. The wave generated by the wave maker can be seen to travel the length of the tunnel and arriving at each wave gauge with the time delay to be expected based on the wave celerity. Within a few wave cycles after the start of the wave energy converter, the amplitude at the down–wave wave gage is greatly reduced, while the wave height at the up–wave wave gage is virtually unchanged.

Analysis of data acquired after the system had reached a periodic state, i.e. after $t = 20s$, was performed using a Fourier transform. The results for both wave gages are shown in figure 9. The harmonic wave present in the up–wave data at half the period of the fundamental wave was consistent with the fact that at this wave height a Stokes wave was expected and observed. On the down–wave side, both the
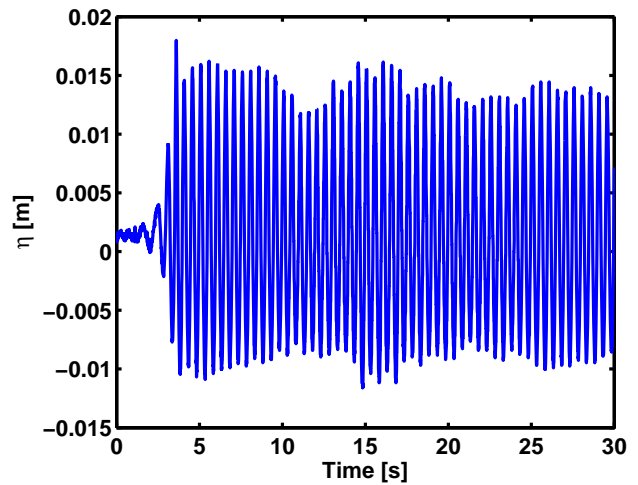
Fig. 7. Up–wave water surface during feedback controlled wave cancellation. For experimental parameters see caption figure 5
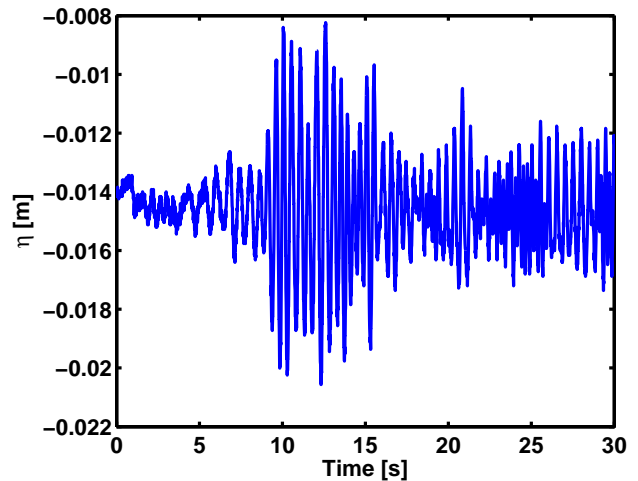
Fig. 8. Down–wave water surface elevation during feedback controlled wave cancellation. For experimental parameters see caption figure 5
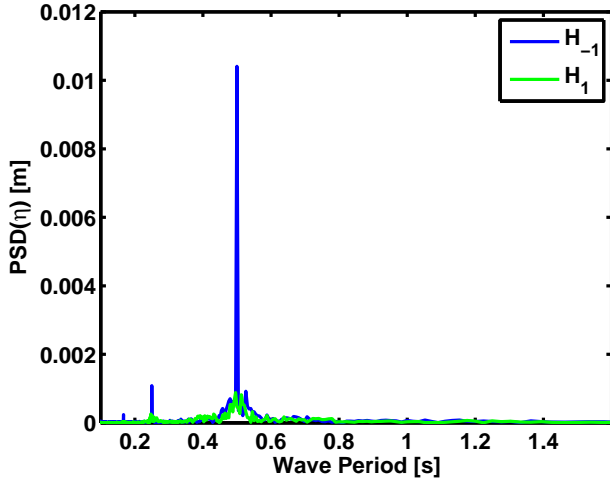
Fig. 9. Power Spectral Density of the surface elevation at the up–wave and down–wave wave gage. For experimental parameters see caption of figure 8
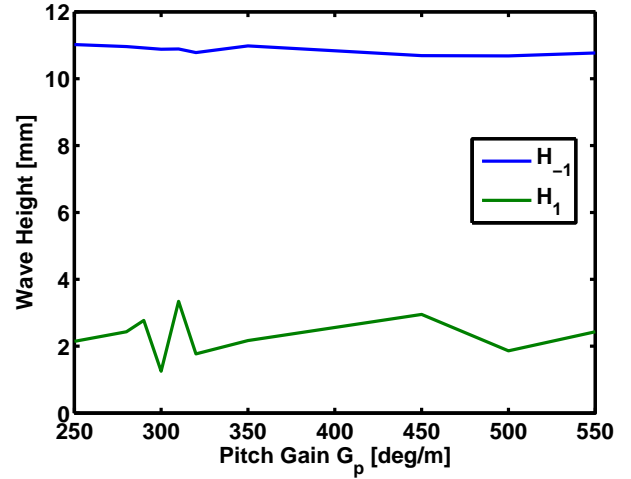
Fig. 11. Fundamental wave heights as a function of blade pitch gain G_p. Incoming wave period $T = 0.5s$, WEC has two blades, feedback phase $\theta = 197°/m$, submergence $|y_c| - R = 10mm$.
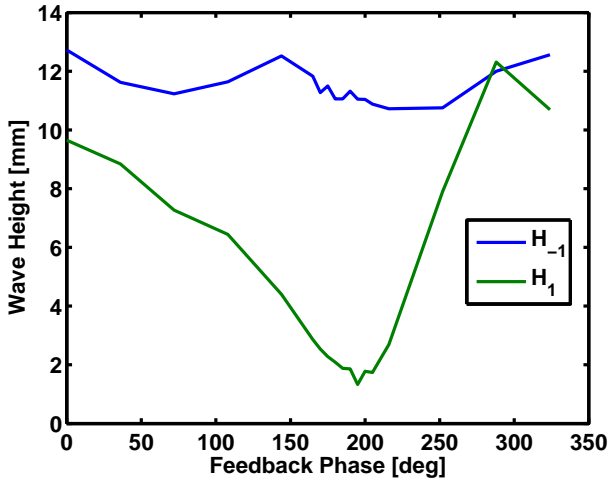
Fig. 10. Fundamental wave heights as a function of feedback phase θ. Incoming wave period $T = 0.5s$, WEC has two blades, blade pitch gain $G_p = 400°/m$, submergence $|y_c| - R = 10mm$.

fundamental and higher harmonic waves were greatly reduced in amplitude. Analysis of the magnitude of the peaks in the Fourier analysis was used throughout the remainder of this paper to quantitatively analyze the efficiency of the wave energy converter.

B. Controller Parameter Optimization

For optimal efficiency, two parameters in the present control approach were adjustable. These were the feedback phase θ as well as the blade pitch gain G_p. The feedback phase optimization was performed first while keeping the pitch gain constant, the results of this study are shown in figure 10.

It can be seen that there is a strong dependence of the wave cancellation efficiency on the feedback phase, which is defined here as the ratio of the fundamental wave height H_{-1} of the incoming wave measured by the up–wave wave gage,

compared to the remaining wave height of the fundamental wave measured by the down–wave wave gage, H_1. While H_1 is smaller than H_{-1} for almost all cases indicating power being extracted from the wave, efficient wave cancellation is only achieved for a small range of feedback phase angles around $\theta = 197°$. In these cases, however, the wave height is reduced by more than 80%. This indicates a wave cancellation efficiency in terms of wave power of more than 95% due to the quadratic relationship between wave height and wave power. The effect of the feedback phase on the incoming wave height H_{-1} can be seen to be small, indicating that in all cases only minor waves traveling in the opposite direction of the incoming wave are generated by the CycWEC. Based on the results shown in figure 10, the feedback phase was fixed to $\theta = 197°$ for the remainder of the results presented.

The effect of the pitch gain G_p on the performance of the CycWEC was investigated next. Figure 11 shows the parameter study where the feedback gain was varied from $G_p = 250 deg/m$ to $G_p = 550 deg/m$ while keeping all other parameters constant.

The height both up–wave and down–wave was almost constant over the entire range of pitch gains investigated. This indicated that the CycWEC is relatively insensitive to pitch gain changes, and a pitch gain of $G_p = 400$ was chosen and kept constant for all further results presented.

C. Wave Height and Period Parameter Study

After the controller had been optimally tuned for the design wave, a parameter study was performed to determine if the CycWEC was able to efficiently cancel waves other than the design wave with a period of $T = 0.5s$. A typical result for varying the incoming wave height by means of adjusting the flap wave maker amplitude is shown in figure 12. While the wave height of the remaining wave down–wave of the CycWEC remained small up to a flap angle of about $2.75°$,
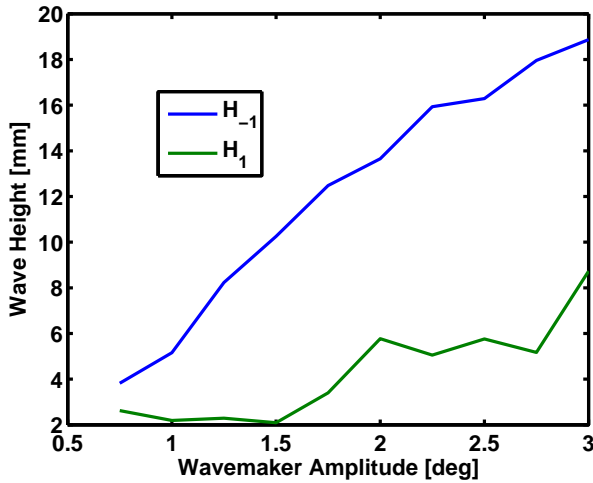
Fig. 12. Fundamental wave heights as a function of flap wave maker amplitude δ. Incoming wave period $T = 0.588s$, WEC has two blades, feedback phase $\theta = 197°/m$, submergence $|y_c| - R = 10mm$.

Fig. 13. Wave cancellation efficiency as a function of flap wave maker amplitude δ. and wave period T. WEC has two blades, feedback phase $\theta = 197°/m$, submergence $|y_c| - R = 10mm$.

a marked increase could be seen beyond this angle. The incoming wave height at this flap angle was about $17mm_{pk}$, and the hydrofoils reached their peak lift generating capability at this wave height. Beyond this wave height, the system was thus limited by hydrofoil stall and could not cancel the entire incoming wave any more.

The results from the entire study varying both wave height and wave period were summarized in the contour plot shown in figure 13. The figure showed the difference between wave power up–wave and down–wave of the CycWEC as a percentage of the incoming wave power. While the performance of the CycWEC deteriorated at the extremes of the investigated parameter space in all directions, the efficiency was mostly flat over a large range of operating parameters. This indicated the capability of CycWEC as well as estimation and control scheme employed to efficiently interact with waves of different height and period.

V. CONCLUSION

We present wave cancellation results for a Cycloidal Wave Energy Converter (CycWEC) model in a 1:300 scale wave tunnel experiment. The wave energy converter was operated under feedback control using a wave gage signal as input for a wave estimator and CycWEC controller. An initial parameter study was performed to tune the controller parameters feedback phase and blade pitch gain, showing sensitive behavior of the CycWEC to mismatches in phase, but robust behavior to changes in pitch gain. The CycWEC was then tested against varying wave heights and periods with the controller parameters kept constant.

Based on the data presented in the preceding section, we conclude that the CycWEC under feedback control is able to efficiently cancel incoming harmonic waves. We were able to demonstrate inviscid conversion efficiencies beyond 85% for a range of wave heights and wave periods around the design
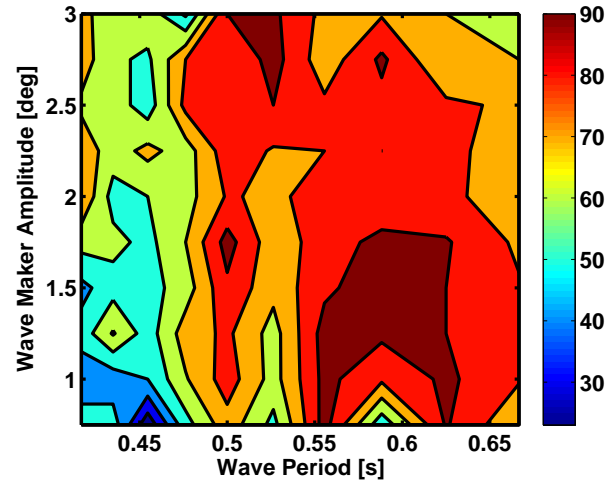
wave of the CycWEC. The efficiency was reduced for wave heights where the blades could not produce larger lift and circulation due to blade stall, as well as wave periods that were further away from the design wave period. The latter behavior was expected based on earlier simulation results that found reduced efficiency once the ratio between wave celerity and blade travel velocity was changed from unity, see Siegel et al. [3] for details.

While the current experiment was limited to indirect wave cancellation efficiency measurements due to its small size, experiments are planned at 1:10 scale for Summer of 2011 at the Texas A&M Offshore Technology Research Center. These will allow for direct shaft power measurements and thus overall efficiency measurements accounting for all losses from wave to shaft. Predictions based on published hydrofoil data, however, do allow an estimate for these losses at less than 30% of the incoming wave power; see again Siegel et al. [3] for details.

REFERENCES

[1] G. Boyle, *Renewable Energy - Power for a sustainable future*. Oxford University Press, 2004.
[2] R. Bedart, "Final summary report - offshore wave power feasibility demonstration project," E2I EPRI Global, WP 009 - US Rev 1, Tech. Rep., 2005.

[3] S. G. Siegel, T. Jeans, and T. McLaughlin, "Deep ocean wave energy conversion using a cycloidal turbine," *Applied Ocean Research*, vol. accepted and in press, 2011.

[4] D. V. Evans, "A theory for wave-power absorption by oscillating bodies," *J. Fluid Mech.*, vol. 77, no. 1, pp. 1–25, 1976.

[5] A. Betz, "Das maximum der theoretisch möglichen ausnützung des windes durch windmotoren," *Zeitschrift für das gesamte Turbinenwesen*, vol. 26, p. 307309, 1920.

[6] S. H. Salter, "World progress in wave energy-1988," *International journal of ambient energy*, vol. 10, no. 1, pp. 3–24, 1989.

[7] D. V. Evans, D. C. Jeffrey, S. H. Salter, and J. R. M. Taylor, "Submerged cylinder wave energy device: theory and experiment," *Applied Ocean Research*, vol. 1, no. 1, pp. 3–12, 1979.

[8] S. G. Siegel, "Cyclical wave energy converter," *U. S. Patent 7,686,583 and pending / awarded International Patent applications*, filed in 2006, awarded 2010.

[9] A. J. Hermans, E. van Sabben, and J. Pinkster, "A device to extract energy from water waves," *Applied Ocean Research Computational Mechanics Publications*, vol. Vol. 12, No. 4, p. 5, 1990.

[10] S. Siegel, M. Roemer, J. Imamura, C. Fagley, and T. Mclaughlin, "Experimental wave generation and cancellation with a cycloidal wave energy converter," in *30th International Conference on Ocean, Offshore and Arctic Engineering (OMAE)*, no. OMAE2011-49212, June 2011.

[11] W. Seelig, "Wave reflection from coastal structures," in *Proceedings of Coastal Structures*. American Society of Civil Engineers (ASCE), 1983, pp. 961–973.

[12] J. Cruz, *Ocean wave energy: current status and future prepectives*. Springer-Verlag, 2008.

[13] S. Siegel, J. Seidel, and T. McLaughlin, "Experimental study of aero-optical distortions in a free shear layer," in *AIAA Paper 2009-0361*, 2009.